# Shipborne lidar investigations of aerosol fields in the atmosphere over Lake Baikal. Part 2. Cross sections

**Yu.S. Balin, A.D. Ershov, and I.E. Penner**

*Institute of Atmospheric Optics,*
*Siberian Branch of the Russian Academy of Sciences, Tomsk*

Received March 24, 2003

This paper presents some results of the lidar investigations into the altitude structure of aerosol fields based on the array of data obtained during the shipborne research mission on Lake Baikal in July–August of 2002. By analyzing the aerosol field cross sections we have revealed a significant effect of local orography on the formation of the field structure. Besides, local features in the spatial aerosol distribution were determined and frequency characteristics of the lee waves were estimated. It was shown that the effect of a mountain ridge on the formation of aerosol field is most pronounced in the central part of the lake with higher mountains on its banks. Here we observed wave motions of two scales along the entire ship route. In the southern part of the lake, small-scale perturbations that are formed behind the ridge spread only up to the central part of the lake. The characteristic feature of the low-frequency atmospheric oscillations is that a linear frequency trend (increase of the oscillation frequency in the direction from the west to the east) occurs.

## Introduction

The results of laser sounding of the atmosphere with a LOZA–M single-frequency lidar[2] obtained during lengthwise routes of Research Vessel *G. Titov* along the coastal line were considered in the first part of the paper.[1] It was noted that orography of the region where measurements had been carried out essentially affects the formation of the spatial structure of aerosol field. Qualitative and quantitative assessment of the effect of the coastal landscape was performed assuming geostrophic transfer of air masses.

The purpose of this paper is the study of cross sections (from one coast to another), in order to more completely describe the formation of a two-dimensional distribution of atmospheric aerosol over the water area of Lake Baikal. Air circulation depends on the wind regime, heat and water budget. Local winds blowing both lengthwise ("barguzin," "verkhovik," etc.) and transverse ("sarma," "kharaikha," etc.) directions essentially affect the wind regime. Also, breeze is observed over Lake Baikal, the coastal breeze is better pronounced.[3] The phenomenon of specific air circulation inside the hollow has been discovered comparatively recently.[4] It lies in directed air motion along the lake perimeter (from north to south on the west coast and from south to north on the east coast).

The authors of Ref. 5 have shown that this type of air circulation is only possible at the presence of stable eastward transfer. The parameters of heat and water budget as well as wind regime show strongly pronounced dependence on the peculiarities of the landscape structure. Cyclonic air mass circulation in the southern part of Baikal is caused by low mountain relief of Olkhinskoe plato and is characterized by wet summer and snowy winter. Rain shadow is dominant to the north of Angara (it is better pronounced near Ol'khon). It is caused by the Primorskii ridge arrangement along the coast and predominant air mass transfer from the northwest. Dry summers and snowless winters are often observed here, that is in sharp contrast with the upper Lena and Angara situated on the west slopes of the same ridge.

## 1. Spatial structure of aerosol fields assessed from the data of laser sounding along the cross-lake directions

The data on spatial distribution of the aerosol field obtained from the vessel moving across the middle and southern parts of the lake were selected for analysis. Time, day, and scheme of the vessel routes are shown in Fig. 1.


**Fig. 1.** The chart of the routes of Research Vessel *G. Titov*. Direction of motion of the vessel is marked by arrow. The date and time of the experiment are shown in the figure.

0235-6880/03/07 541-11 $02.00 

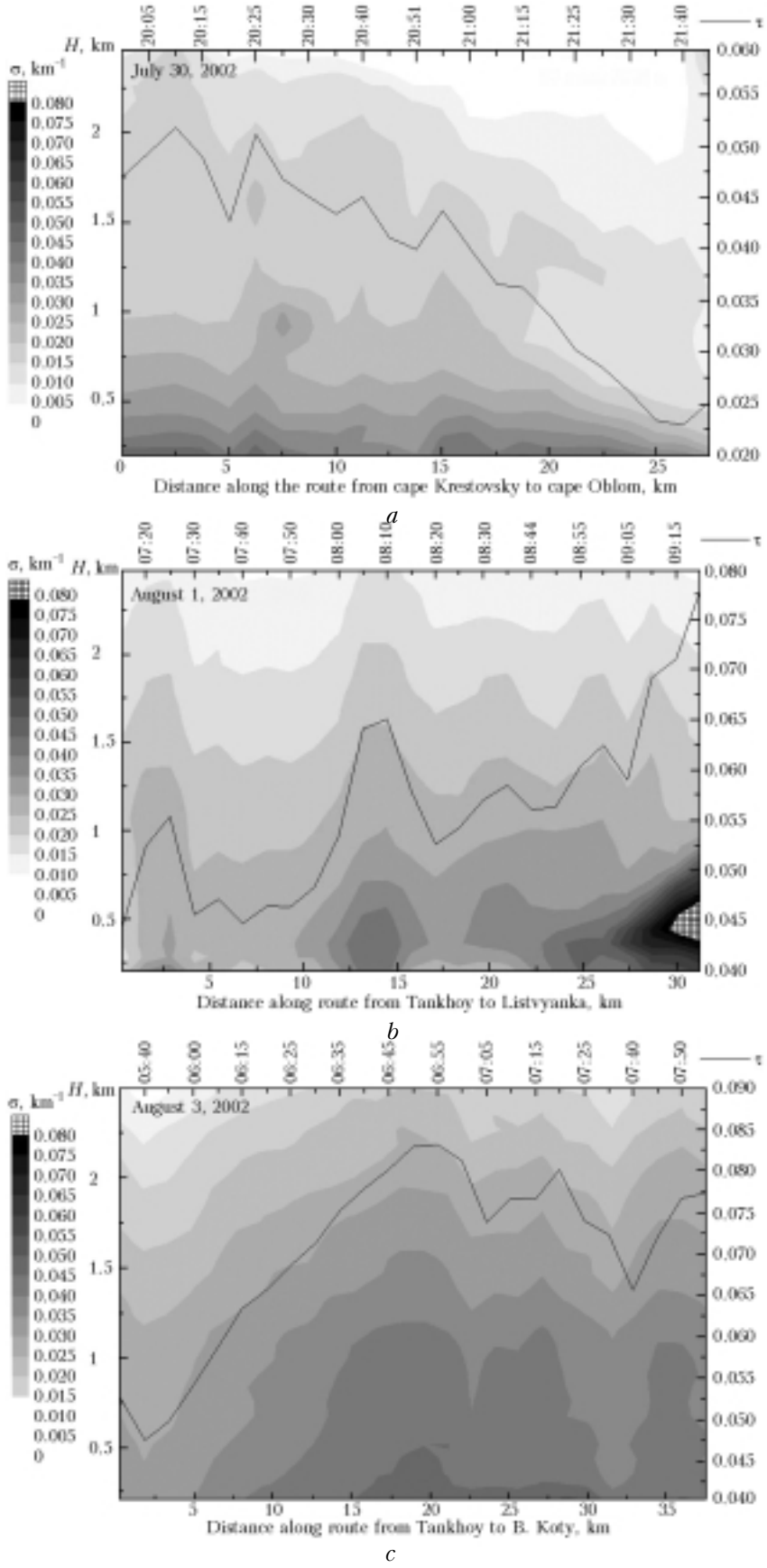


**Fig. 2.** Spatial cross sections of the aerosol scattering coefficient obtained on July 30 (*a*), August 1 (*b*), and August 3 (*c*) 2002.

Synoptic conditions during the period of observations were the following: anticyclone prevalent over the region moved to the east on July 29–30, and it was replaced with a low-gradient field of enhanced pressure, which determined weather conditions until July 30 when the pressure field was transformed and replaced with low-gradient field of low pressure. The continental midlatitude air mass determined temperature and humidity regime. Anticyclone determined weather in the region on August 1, in this connection the wind from the northwest blowing at a speed of 2–3 m/s was observed. Then the anticyclone was gradually destroyed, and the low-gradient field of enhanced pressure was formed. It determined the weather in the region approximately until 11 a.m. on August 3.

The sounding results are shown in Fig. 2, where the value of the scattering coefficient is presented by the distribution of blackening on the brightness scale, the values of the optical thickness $\tau(0.2–2.5$ km) are also shown here. Figure 2*a* shows the route from cape Krestovskii to cape Oblom, Figs. 2*b* and 2*c* show the routes Tankhoi–Listvyanka and Tankhoi–Bol'shie Koty, respectively.

The decrease of the optical thickness from the west coast to the east is characteristic of the spatial distribution of optical characteristics of the atmosphere over the middle part of Lake Baikal (Fig. 2*a*). Let us consider, what processes in the atmosphere should determine the aerosol spatial distribution during the experiment. Disturbance of the principal airflow by the mountain ridge favors the formation of zones of descending and ascending airflows and, hence, the areas with different optical characteristics. Vertical distributions of wind velocity and direction also affect the stratification of the aerosol scattering coefficient. Westward wind with the velocity of 4 m/s was observed in the near-water layer of the atmosphere during measurements at the west coast, then as the vessel moved to the east, wind became southward and its speed decreased to 3 m/s. The principal airflow over the mountains propagated mainly to the west at a speed of 5 m/s.

According to data from Ref. 6, the northern part of Lake Baikal is characterized by very clean atmosphere. The extremely low aerosol concentrations were recorded at weak southward wind in the near-surface layer of the atmosphere in the region of Middle Baikal. Hypothetically, several factors determined the spatial pattern of aerosol field on July 30. They were: coming of air masses with lower content of aerosol particles to the near-ground layer of the atmosphere from the northern part of Lake Baikal; the process of transfer of the continental midlatitude air mass with the principal airflow; deformation of the airflow by mountain ridge with the formation of leeward waves which gradually damped while moving out of the ridge.

The spatial section of the aerosol field in the southern part of Lake Baikal was obtained on August 3 under conditions of the low-gradient field of enhanced pressure (Fig. 2*c*). As follows from analysis of synoptic situation, significant instability of the atmosphere was observed during this time. Meteorological measurements onboard the vessel showed the presence of northeast wind (along the coast) at a speed of 4 m/s in the eastern part of the route, and calm was observed in the middle of the lake and later. The principal airflow kept westward direction. Thus, the processes similar to the aforementioned ones are observed in the east part of the lake, and the processes of convective air motions with developed air mixing characteristics of neutral stratification of the atmosphere determine the pattern of aerosol field in the middle and western parts of the spatial cross section.

The data obtained on August 1 along the route from Tankhoi to Listvyanka are interesting as, first, they were obtained under conditions of low relief of the west coast, and, second, it is the most essential, that they should represent the effect of the sources of industrial aerosol from industrial centers along Angara river at the air mass transfer from the northwest. The conditions of low relief should provide relatively uniform vertical distribution of aerosol in the horizontal plane on the major part of the route. Such a pattern in observed in Fig. 2*b*. It shows an essential increase of $\tau(0.2–2.5$ km) at the source relative to analogous values in the beginning of the route near the opposite coast. As is seen in the figure, the lower 700-m layer makes the greatest contribution to these variations. In addition, it follows that the effect of admixtures on the structure of aerosol field is prolonged to the depth of 5 km from the coast, and then relatively uniform horizontal distribution of $\sigma(H, L)$ is observed.

Similar pattern of increase of the aerosol concentration near the source of Angara river was observed in Ref. 6 from the results of long-term measurements in the near-surface layer of the atmosphere during shipborne missions. It was also shown there from the data of photoelectric laser analyzer that the number density of suspended particles strongly depends on the wind direction. The aerosol number density increases twice, on the average, under prevalent winds from the northwest.

Another peculiarity of the latter cross sections is a noticeable increase of the values of aerosol scattering coefficient in the central part of the lake, especially in the lower layer of the atmosphere (up to 400–500 m). One of the possible explanations of this fact could be the following. It was shown resulting from investigation of near-coast streams of Lake Baikal water[7] that two systems of streams are observed. The first is cyclonic in the central part of the lake (between maxima of the near-coast streams), and the second, anticyclonic, is observed in the coastal parts of the lake. The downwelling areas are formed in the region of maximum coastal streams, and the upwelling area is observed in the central part. It affects temperature of the lake surface, that means that the central part of Lake Baikal should be colder.

Authors of Ref. 8 have studied the response of the boundary layer of the atmosphere to the change of temperature of the underlying surface in the hydrological front zone. The local minimum of the heat flux appears at the water surface – atmosphere boundary at transport of relatively warm atmospheric air to the cold underlying surface. The process of transport of heated air is accompanied by appearance of advective fogs just behind the front surface. We did not observe advective fogs during our measurements in the aforementioned days, but they were observed earlier in 2001 while working at the coast.

Similar processes occurring in the central part of the lake, probably, lead to humidification of aerosol and, hence, to the increase of the value of the aerosol scattering coefficient. The plot of relative humidity measured just onboard the vessel (Fig. 3) favors this assumption.

The increase of the values of relative humidity is observed in central part of the lake in the experiments carried out on July 30 and August 1. Relative humidity of the air exceeded 70% during all the experiment (Fig. 3). The effect of increase of the aerosol particle size was observed at the relative humidity above 60% because of heterogeneous condensation on hygroscopic nuclei, the change in particle size at their condensational growth in the atmosphere occurs much quicker than due to other processes.[9]

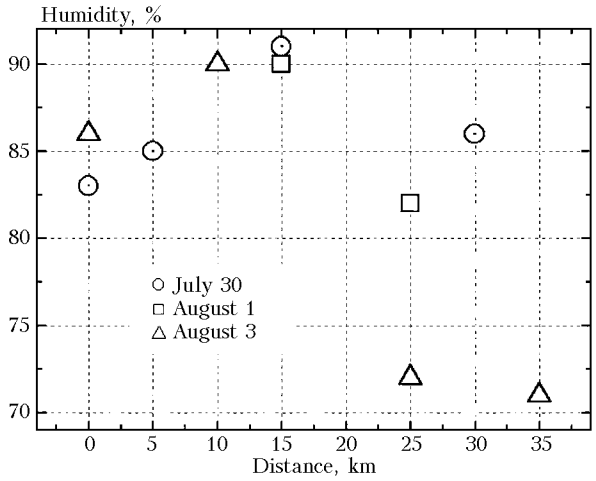


**Fig. 3.** Relative humidity in the near-surface layer of the atmosphere during the experiment.

To qualitatively estimate the relations between the optical parameters of the atmosphere at different heights within the limits of spatial cross section, let us consider the autocorrelation matrices $R(H)$ for the profiles $\sigma(H)$, as was done earlier.[1] The correlation matrices were calculated for the range 0.2 to 2.5 km with the spatial resolution of 130 m.

The autocorrelation functions are shown in Figs. 4*a–c*, the number of profiles used in calculations is also shown here.

As is seen in Fig. 4, in general, the correlation among the data on vertical profiles presented is different. The behavior of the autocorrelation matrices obtained on July 30 and August 1 are similar largely. The correlation coefficient decreases with height approximately to 1 km, then its increase, better pronounced on July 30, is observed up to 1500–1700 m, and then it decreases with height up to 2500 m. The height of the correlation layer is 750 m (Fig. 4*a*) and 1 km (Fig. 4*b*). These values differ from that observed earlier under stationary conditions.[10]

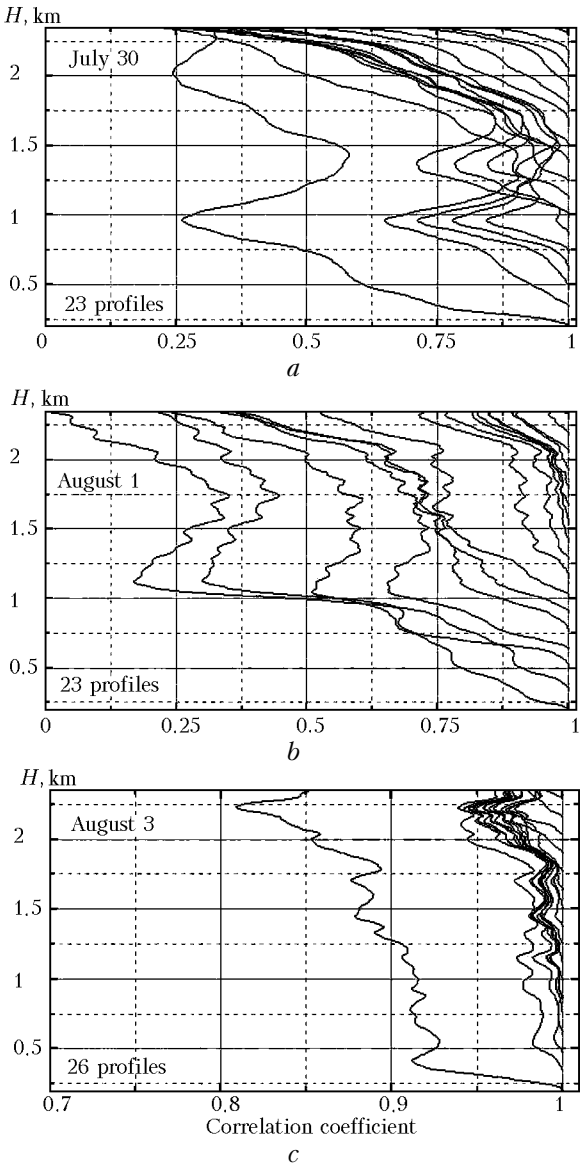


**Fig. 4.** Autocorrelation matrices of the vertical behavior of the scattering coefficient along the cross parts of the vessel route.

Probably, it can be explained for the spatial cross section obtained on August 1 by the fact that the cold front passed over the region under investigation just during the measurements, and the

midlatitude air mass was replaced with the Arctic one. The presence of well pronounced boundary at a height of 1000 m in the data obtained on July 30, where the increase of the autocorrelation is observed at the height of 1500 m, is most likely caused by the effect of orography, because the height of the jump coincides with the height of the mountain ridge.

The autocorrelation matrix shown in Fig. 4*c* is essentially different from that shown in Figs. 4*a*, and *b*. Very high values of the correlation coefficient at all heights are observed here. Taking into account that the route on August 3 is close to that on August 1, as was mentioned above, one can explain these high values by the fact that significant instability of the atmosphere was observed in this time (strong vertical motions and mixing).

As was noted in our previous paper[1] devoted to the lengthwise sections, the obvious spatiotemporal nonstationarity is observed in the behavior of the aerosol field along the entire route of the vessel. So the apparatus of continuous wavelet transform (CWT) is applicable of providing a more detailed analysis of the spatial cross sections of the aerosol field. The principles of CWT are briefly described in the Appendix.

## 2. Application of CWT to processing the cross sections of aerosol field

The most long (about 250 km) vertical section of the aerosol field in the atmosphere over Lake Baikal was obtained on July 31 – August 1, 2002 along the coastal line and analyzed in our previous paper.[1] Essential nonstationarity of the process of fluctuations of the optical characteristics of the atmosphere in the two-dimensional field of the section was also revealed there. It is interesting to consider, what peculiarities of the aerosol field fluctuations become apparent in time, and what spectral characteristics are present. The wavelet spectrogram of the aforementioned longitudinal section of the aerosol field is shown in Fig. 5.

Three time intervals with different spectral characteristics (marked by arrows) can be selected in Fig. 5. These intervals have well-pronounced temporal (spatial) boundaries. The spatial boundaries revealed coincide with the change of the parameter $\xi = \omega H_{\text{mean}} / U$ that characterizes the degree of disturbance of the airflow by an orographic obstacle.[11,12] Here $H_{\text{mean}}$ is the mean height of mountains, $\omega = \frac{1}{2\pi}\sqrt{\frac{(\gamma_a - \gamma)g}{T}}$ is the Brunt-Vaisala frequency, $U$ is the horizontal component of the mean wind velocity, $\gamma$ and $\gamma_a$ are, respectively, the vertical and dry adiabatic lapse rate, $T$ is temperature of the ambient air.

Fluctuations of the aerosol scattering coefficient in the region with the height of coastal mountain ridge above 1500 m have the greatest amplitude, and three characteristic scales (frequencies) of the wavelet-expansion can be isolated. The amplitude of fluctuations decreases on the route part along the ridge that have the height from 1000 to 1200 m, variations of the smallest scale (high frequency) disappear, and only low-frequency component of the wavelet spectrum is observed on the part where the mean height of mountains does not exceed 1000 m. The increase of the number of spectral components in the wavelet expansion of the aerosol field as the value $\xi$ increases is an evidence of that the aerosol field over the lake is formed due to the orography of the region. The wavelet spectrogram considered indicates high efficiency of the wavelet transforms used for investigation of frequency-temporal characteristics of aerosol fields.

The results of applying the CWT to processing the lidar data on cross sections are shown in Fig. 6, where the scale axis is frequency, for convenience.

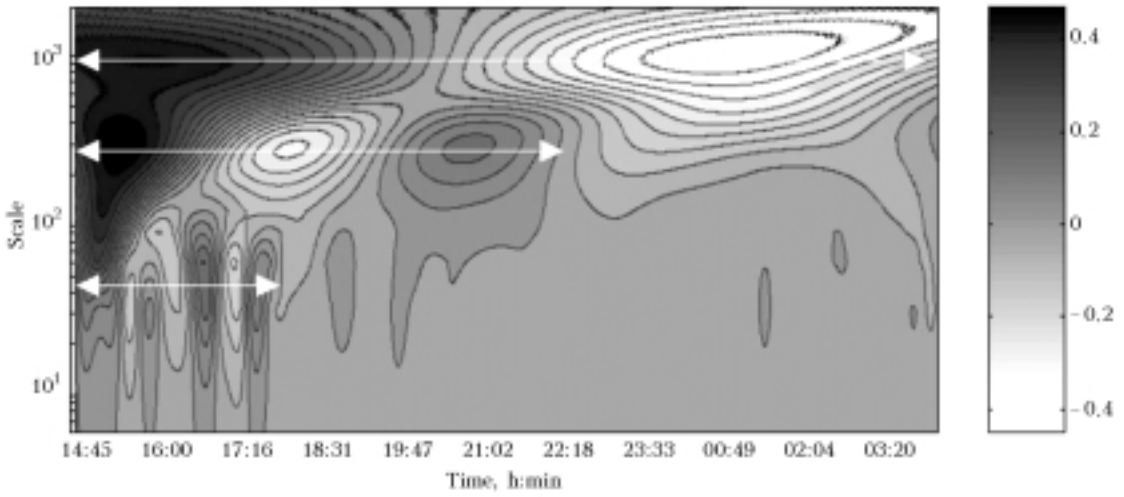


**Fig. 5.** Wavelet spectrogram of the spatial section of the aerosol field on July 31 – August 1, 2002 at the height of 500 m.

The CWT coefficients $C(a, b)$ were calculated at the height levels from 250 to 3000 m. The values $C(a, b)$ in the height ranges demonstrating the most characteristic peculiarities of the data analyzed are shown in Fig. 6. Maximum values of the coefficients of wavelet expansion of the spatial cross section of aerosol field on July 30 at the level of 250 m, the values of which are shown in Fig. 6*b*, are reached on the scale corresponding to the frequency of $2.8\times10^{-4}$ Hz. That means, that the wave has two full oscillations of the period of about 14.5 km on the selected scale. The period of the wave increases as the height increases, and the wave with the period of 30 km is observed at the height above 700 m (Fig. 6*a*), the frequency of this oscillation shows an increase in linear trend and changes from $1\times10^{-4}$ to $1.7\times10^{-4}$ Hz. As the height subsequently increases, the trend is gradually smoothed, and the frequency of $1.15\times10^{-4}$ Hz is best pronounced at the heights above 2000 m.

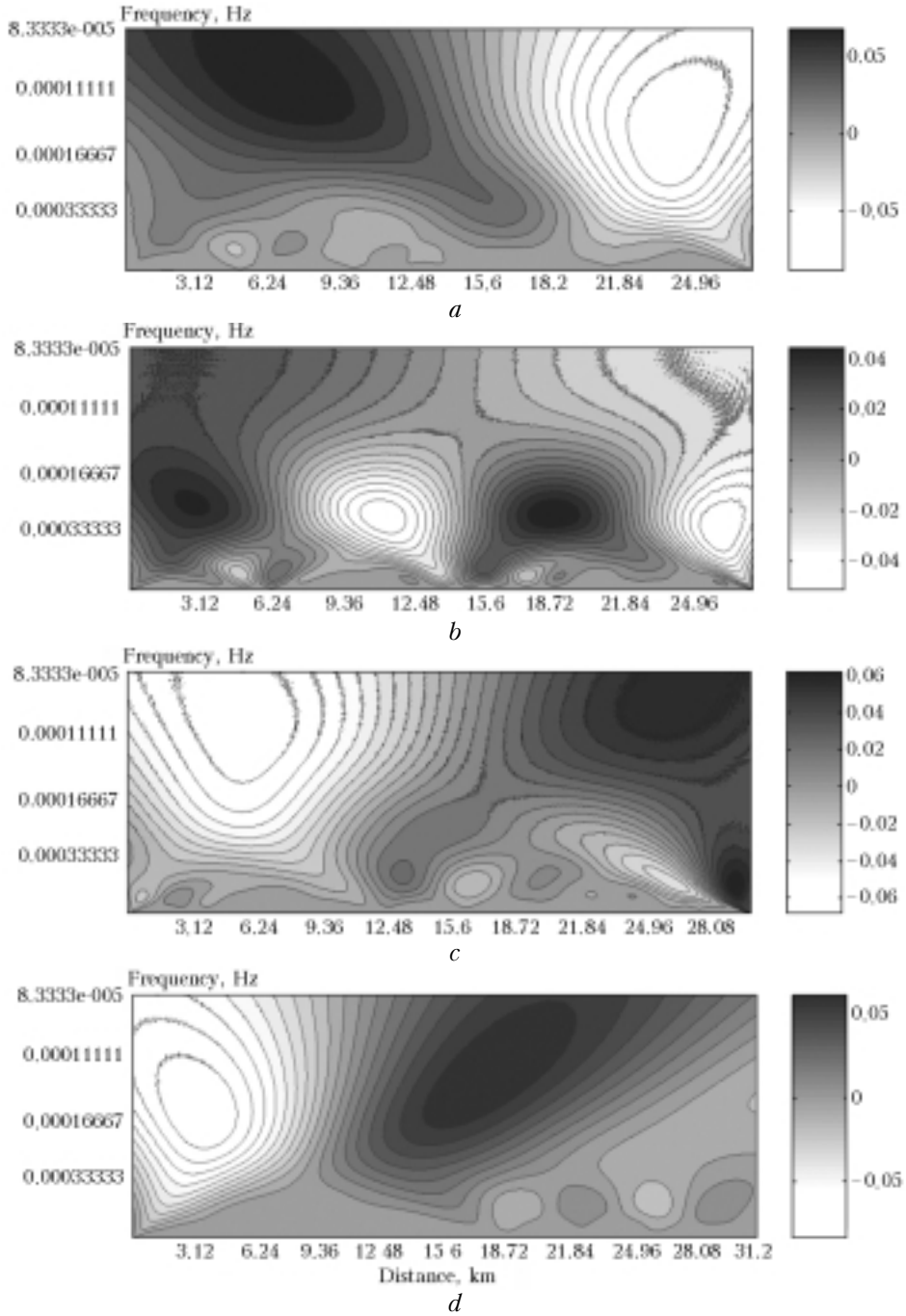


**Fig. 6.** Wavelet spectrogram of the spatial section of the aerosol field at the height of 750 m (*a*) and 250 m (*b*) on July 30, 2002; 750 m on August 1, 2002 (*c*) and 750 m on August 3, 2002 (*d*).

The most typical view of the wavelet expansion of the cross section of aerosol field on August 1, 2002 is shown in Fig. 6*c*. The fundamental frequency, which is present at all heights, takes here a lower value of $9.8\times10^{-5}$ Hz. The wavelet coefficients become more significant at heights below 700 m, which show the local peculiarities of fluctuations of the optical properties of the atmosphere over the central part of the lake and near its west coast. Contribution of inhomogeneities to the spatial pattern of aerosol field in the east part of the route and over the central part of the lake increases above 700 m. Local increase of the scattering coefficient in the center of the section is presented by the increase of the values $C(a, b)$ at all height levels below 3 km.

Oscillations of the aerosol field measured on August 3 weakly change with height, so that only the wavelet spectrogram of a single height level is shown in Fig. 6*d*. The peculiarity is observed at the heights below 2.5 km which lies in the presence of higher frequency of $6.6\times10^{-4}$ Hz on the half of the 15-km long part of the route from the west coast to the middle of Lake Baikal. Similarity of the behavior of the wavelet expansion coefficients is seen in Figs. 6*d* and *a* in the low-frequency range, but the trend has inverse behavior. This is related to the fact that the cross section of this spatial section was performed in the reverse direction.

It is known that the behavior of the wind field essentially affects the spatiotemporal distribution of aerosol in the atmosphere. In its turn, the presence of long mountain ridges on the banks of Lake Baikal affects the behavior of airflow, and, hence, the spatial distribution of aerosol over the lake. For example, two ridges of Primorskii ridge with the heights of 1000 and 1100 m and the distance between tops about 8.5 km are situated in parallel to the lake coast near cape Krestovskii. The ridge heights near village Bol'shie Koty reach 1000 m, and, in our opinion, the orography of the region pronounced as formation of leeward waves should affect the formation of the aerosol field in cross sections.

## 3. The effect of orography on the formation of aerosol field

Motions with horizontal scale of 1 to 100 km, depending on wind velocity and parameter of stability of the atmosphere appear in the airflow over mountains.[12] The condition of appearance of the waves observed down-stream from the obstacle is fulfillment of the inequality

$$l_1^2 - l_2^2 > \left(\frac{\pi}{2H_1}\right)^2,$$

where $l_1^2$, $l_2^2$ are the Scorer parameter[13] values (factor of stability). The parameter $l_2$, according to Ref. 13, is defined as $l^2 = 4\pi^2\,\omega^2/U^2$ and is calculated at different heights $H_1$ and $H_2$, $U$ is the horizontal component of the wind velocity in the layer limited by these heights.

The frequency $\omega = 0.01\ s^{-1}$ for temperature $T = 290$ K and $\gamma = 0.0065$ K/m. According to the synoptic data obtained in the region of Bol'shie Koty and in the region of cape Krestovskii, the values of the wind speed at the heights of 1500 and 3000 m were 3 and 5 m/s, respectively. Hence, the threshold condition of leeward wave formation is fulfilled for the experiments carried out on July 30 on the route cape Krestovskii – cape Oblom and on August 3 on the route from Tankhoi to Bol'shie Koty. It was shown[12] that the leeward wave amplitude depends on the parameter of stability, height and width of the ridge.

The value of the parameter $\xi \approx 1$ under atmospheric conditions realized on July 30 and August 3. In this case the waves appear with alternative horizontal and vertical areas of ascending and descending motions. The wave oscillation amplitude is close to the height of the mountain ridge, and the wavelength can vary within the limits 5 to 30 km with more probable value 10 km. Besides, the effect of wind velocity on appearance of leeward waves behind obstacles is connected with temperature stratification of the atmosphere. As is shown,[12,13] at flowing around the mountain ridge by airflow with unstable stratification, wave phenomena are formed at a low speed of the air flow, and under stable stratification wind velocity should be no less than 8 m/s. The upper limit here is the value 25–30 m/s, when no wave phenomena are observed independent of stratification.

Based on the results obtained with the use of CWT of the cross sections of aerosol field one can suppose that weak plane leeward waves were observed during the experiment. It is explained by low wind in this period. Fluctuations of the scattering coefficient with characteristic frequencies hypothetically caused by the effect of leeward waves were revealed when analyzing the data obtained on July 30 and August 3. Leeward waves were observed during the entire period of measurements on July 30 up to the height of 500 m and on the west side of the spatial section on August 3. The increase of the frequency of occurrence of maxima of the coefficients of wavelet expansion at the increase of the spatial shift agrees with the theoretical calculations, which show that the distance between the wave crests for flow lines decreases down-stream.[11]

The airflow propagating over mountains has its own (natural) wavelength, which depends on the spatial distribution of horizontal gradients of the meteorological quantities.[14] The fundamental frequencies considered in section 2 of this paper varied from $9.8\times10^{-5}$ to $2.8\times10^{-4}$ Hz, more likely, correspond to the natural frequencies of the airflow. Orographic effect is observed here only in the appearance of a small trend in the height range from 750 up to 2000 m. Unstable stratification of the atmosphere observed on August 3 also didn't favor

the formation of leeward waves. It is known that the stable atmosphere is favorable for leeward waves, when the waves of small duration and high amplitude exist, because the great stability increases the return effect of gravity force on moving air.

There is a local minimum of the optical thickness on the spatial cross sections obtained on July 30 and August 3. The minimum is in the west part at about 5-km distance far from the section boundary. It is the result of down-stream propagation of the initial disturbance caused by deformation of the flow by obstacles and, most likely, corresponds to the area with the absence of vertical motions of air masses.[15]

On the whole, the results of wavelet analysis of the spatial cross sections of aerosol field obtained on July 30 and August 3 well agree with the theoretically calculated data on the lee waves.[12,13]

## 4. Estimation of the effect of anthropogenic aerosol sources

Traditionally, the region of Lake Baikal is considered as a "background" region, i.e., significant amount of aerosols is formed resulting from natural processes, with small admixture of pollutants. Atmospheric transparency over the lake is, on the average, 13% higher than that over Irkutsk.[3] Visually, the air over Baikal enables one to discern the mountain summits at 200-km distance and farther. At the same time, the presence of Irkutsk industrial zone, enterprises of Baikalsk and Slyudyanka just near the lake favor the accumulation of admixtures near the local sources,[16] and transfer of aerosol to the lake area is possible at winds with strong monsoon component or developed circulation inside the hollow. In order to study such a possibility of anthropogenic effect on the lake, special experiment has been carried out. Sounding was carried out at the south edge of the lake on the route Baikalsk–Kultuk, where Baikalsk Pulp and Paper Mill is the main source of pollution. According to the materials of the Complex Scheme of Preservation of Environment over the Territory of Lake Baikal and "National report of the USSR to UN Conference in 1992 on the environment and development," this region is included into four areas of pernicious anthropogenic effect on ecological systems of the region.

According to data from Ref. 6 the probability of industrial emissions of BPPM is from 10 to 100%. The upper estimate of the mean annual emission settling on the lake water area reaches 50%, the area of the zone of spread of pollutions is, on the average, 400 km$^2$ (for comparison: the probability of settling of industrial aerosol from Irkutsk–Angarsk industrial center does not reach 4%, while the area of spread of pollutions in 2800 km$^2$).

The results of the experiment conducted are shown in Fig. 7. Measurements were carried out under conditions of stable anticyclone; wind in the near-surface layer blew prevalently from the south direction at a speed no more than 1 m/s. The enhanced aerosol concentration as compared with the background one was observed at the heights from 350 to 500 m. This aerosol had obviously industrial origin being the product of a BPPM atmospheric emission.

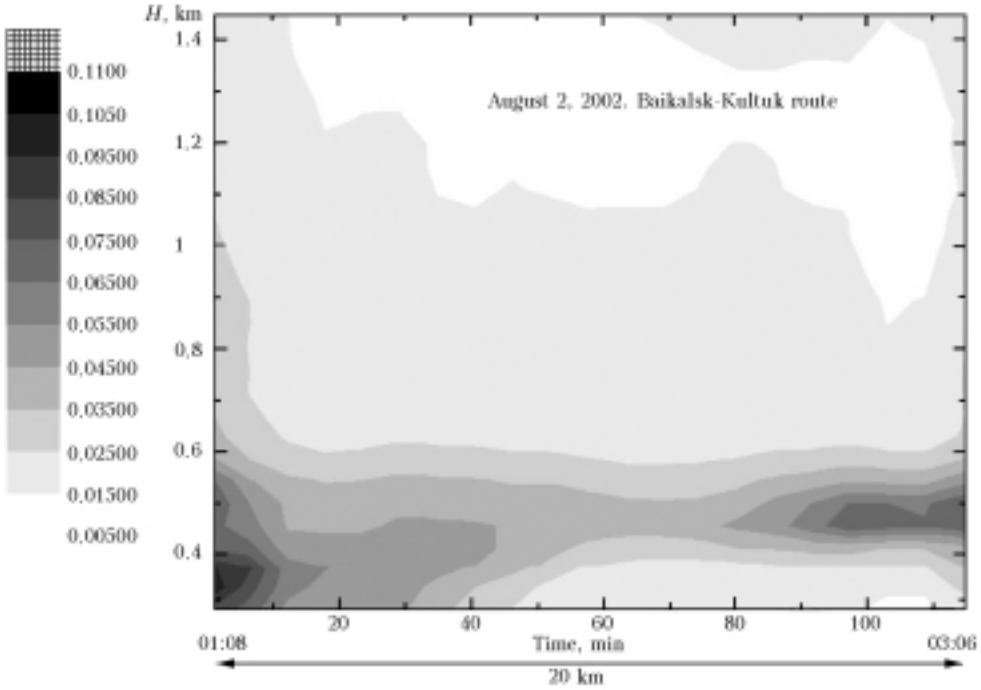


**Fig. 7.** Spatial structure of the aerosol scattering coefficient along the coastal line along the route from Baikalsk to Kultuk.

Anticyclonic conditions and weak south wind favored the spread of the emission plume along the coastal line limited by the Khamar-Daban ridge from south and southwest. Minimum in the middle part of the plume corresponds to the farthest point of the plume from the lidar. The fact that the plume of emission is observed at the distance of more than 20 km from the local anthropogenic source enables us to conclude that the effect of BPPM on the south part of the lake is significant.

## Conclusion

As was noted,[17] simulation of the processes of atmospheric pollution in the region with complex orography is connected with the necessity of calculating (or reconstructing from the data of measurements) of inhomogeneous fields of meteorological elements and turbulent characteristics in the boundary layer of the atmosphere over nonuniform underlying surface. This problem is especially difficult if stated for local and mesoscale, when the network of meteorological stations is insufficiently dense. In this case the most acceptable way for calculating the fields of distribution of optical and meteorological characteristics of the atmosphere is construction of the model of the dynamics of the atmosphere together with solving the problem on transfer of the admixtures. The tear-off lee and wave motions behind mountain ridges and in mountain valleys can play important role in the atmospheric flows under conditions of complex orography, when vertical and horizontal scales are comparable. The lidar experiment enabling one to study the structure of aerosol fields with good spatial and temporal resolution makes it possible to verify the models of dynamics of the atmosphere. The study of spatial cross-sections of the aerosol field using CWT and correlation analysis enables us to reveal some peculiarities. The height level, above and below which the behavior of the wavelet coefficients is different, is close to the height of correlation, which can be accepted to be equal to the height of mixing layer.[24]

The effect of mountain ridge on the formation of aerosol field, lying in the formation of lee waves is well pronounced in the middle part of the lake that has higher banks. Wave motions of two scales are observed here along the entire route of the vessel motion. The small-scale disturbances formed behind the ridge in the southern part of the lake spread only to the middle of the lake. The characteristic peculiarity of low-frequency atmospheric oscillations is the presence of linear frequency trend (the increase of the frequency of oscillations when moving the vessel from west to east).

### Acknowledgments

The work was supported in part by Russian Foundation for Basic Research (Grant No. 02–05–64486), INTAS 01–0239, and CRDF RG2–2357–TO–02.

### Appendix

## Principles of wavelet analysis

Wavelet analysis has been developed in solving the problems of analysis of peculiarities of complex signals of different scales. The method of CWT is based on the expansion of a signal in Gilbert space over the basis of functions fulfilling certain requirements by means of changes and shifts of scale. Such transform makes it possible to realize continuous wavelet analysis of the signal in the scale–shift field (frequency – time).

The coefficients of the direct CWT are calculated by the formula[18,19]:

$$C(a,b) = \frac{1}{\sqrt{a}} \int_{-\infty}^{\infty} s(t)\,\psi\left(\frac{t-b}{a}\right) \mathrm{d}t,$$

where $s(t)$ is the signal to be analyzed, $\psi(t)$ is the wavelet function, $a$ and $b$ are the parameters of scale and shift, $a \in R^+$, $b \in R$, $\psi \in L^2(R)$. The parameter $b$ sets the wavelet position determining its temporal or spatial location. The value of the parameter $a$ determines the scale and provides the frequency localization by compressing and/or stretching. In fact, it is an analogue of frequency in the Fourier transform. Thus, the function $C(a, b)$ for each pair of $a$ and $b$ determines the amplitude of the corresponding wavelet.

If the wavelet function $\psi$ has satisfied the condition of permission,

$$K_\psi = \int_{-\infty}^{\infty} \frac{|\,\bar{\psi}(\omega)\,|^2}{\omega}\,\mathrm{d}\omega < \infty,$$

where $\bar{\psi}(\omega)$ is the Fourier-image of the wavelet, then reconstruction of the signal is made by the following relationship:

$$s(t) = \frac{1}{K_\psi} \iint_{R^+ R} C(a,b)\, a^{-\frac{1}{2}}\, \psi\left(\frac{t-b}{a}\right) \frac{\mathrm{d}a\mathrm{d}b}{a^2}.$$

The peculiarity of the wavelet function lying in frequency-temporal location enables one to follow the temporal (spatial) change of the spectral properties of the signal analyzed. It is the principal advantage of CWT over the Fourier analysis for revealing the peculiarities of the series of data. Such peculiarities are, for example, evolution of the frequency spectra of the signal, the moments of local changes of the amplitude of characteristics, calculation of different fractal characteristics of the signal, etc.

Following the Heisenberg uncertainty principle, in scaling the wavelet, the area of cells on the phase plane time–frequency remains constant after stretching. That means that wavelets well localize the low-frequency components of the analyzed signal in the frequency range, and high-frequency in the time range (it is very convenient when processing real signals where low-frequency components have

significant extension, and high-frequency, as a rule, are small).

The advantages of wavelet transform over the window Fourier transform lies in automatic reduction to the effective temporal (or spatial) window adjusted to the signal analyzed, i.e., to its fundamental frequencies (scales).[20,23] This property of "mobility" of the frequency-temporal window of CWT enables one to reveal equally good both low-frequency and high-frequency characteristics of signals,[18] while the Fourier transform is more suitable for analysis of the signals with well distinguished frequency components and does not provide for clear idea of close frequencies.

The wavelet function should fulfill the following conditions: space limits; location, i.e., the presence of compact carrier in both temporal and spatial ranges of definition of the function; zero mean value. The wavelets based on Gaussian functions, "Mexican hat" wavelet, DOG wavelets (difference of two Gaussian functions), Morle and Dobeshi wavelets have received wide acceptance for continuous wavelet analysis. The choice of analyzing wavelet is determined by information that should be extracted from the data series.[18] The general rule in practice is that the form of the wavelet should be similar to the form of the data analyzed.[23] One of the most popular and widely used wavelet "Mexican hat" is used in this paper for analysis of the lidar data. It is defined as second derivative of the Gaussian distribution density of a random process:

$$\psi(t) = \frac{2}{\sqrt{3}}\pi^{-\frac{1}{4}}\left(1-t^2\right)e^{-t^2/2}.$$

The advantages of this type of the mother wavelet are the presence of more compact carrier (central frequency is equal to 0.25 Hz),[21] smoothness and symmetry, simplicity of calculation, that quickens the work of CWT. More narrow Fourier spectrum of "Mexican hat" determines better frequency resolution as compared with other wavelet functions.

To make sure, let us consider the following example. Let the signal $s(t)$ (Fig. 8*c*) be set in the form of a sum of signals $s_1(t)$ (Fig. 8*a*) and $s_2(t)$ (Fig. 8*b*), where $s_1(t) = \sin(2\pi f_0 t^2)$, $s_2(t) = \sin(2\pi f_1 t)$ on the first half of the signal duration,

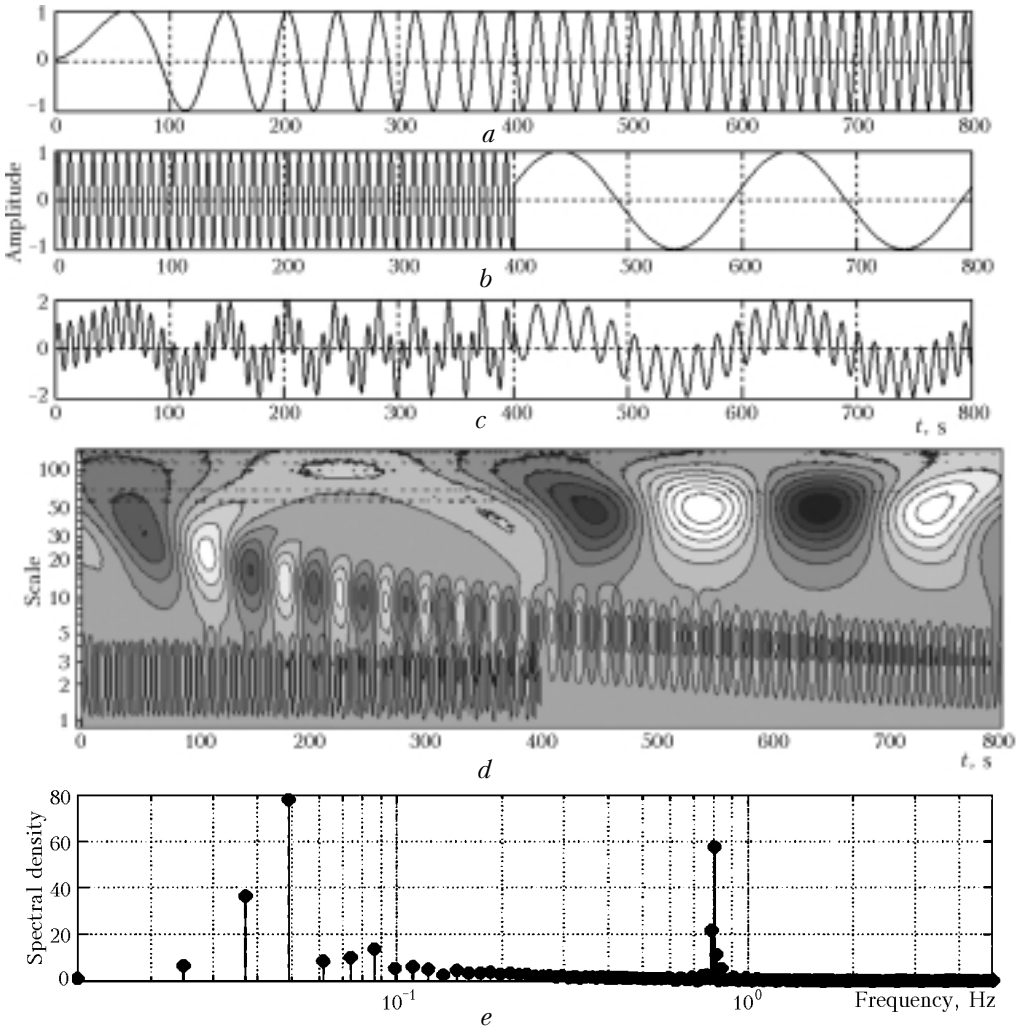


**Fig. 8.** Components of the analyzed signal (*a*, *b*); total signal (*c*), wavelet spectrum of the signal under study (*d*), spectral density constructed based on the fast Fourier transform (*e*).

and $s_2(t) = \sin(2\pi f_2 t)$ on the second half of the interval. Let us set the frequencies $f_0$, $f_1$, and $f_2$ equal to 0.005, 1, and 0.05 Hz, respectively. The values of the expansion coefficients $C(a, b)$ are shown in Fig. 8*d* in the gray scale. It is well seen in Fig. 8 that CWT provides for a comprehensive picture of the dynamics of the temporal variations of the frequency characteristics. Three spectral components of the signal are well distinguished. The low-frequency oscillations at wavelet transform have more large scale, and high-frequency oscillations have smaller scale. Three characteristic values of the maxima of energy of the wavelet spectrum can be selected on the logarithmic scale: 2.5 in the first part of the signal duration, 50 in the second part and the scale present on all durations and varying from 40 to 3. Determination of the frequencies of harmonics after determination of the characteristic scales is reduced to simple recalculation of these values into frequency by the formula[22]:

$$f = f_\psi/(a\Delta t),$$

where $f_\psi$ is the frequency of the central splash of the wavelet (Hz), $\Delta t$ is the discrete step, $a$ is the recalculated value of the scaling variable. At substitution taking into account $f_\psi = 0.25$ (the "Mexican hat" wavelet was used in the expansion), $\Delta t = 0.1$, we obtain the initial frequencies of the signals of 1 and 0.05 Hz, as well as the frequency varying from 0.06 to 0.8 Hz. This example is an evidence of the fact that the wavelet transform is essentially more informative as compared with the Fourier transform, where only the frequencies of the signal $s(t)$ equal to 1 and 0.05 Hz are revealed (Fig. 8*e*). A false idea can be obtained from the form of the Fourier transform of the existence of these frequencies on the entire time interval. Information about the component of the initial signal $s_1(t)$ is lost.

## References


1. Yu.S. Balin, A.D. Ershov, and I.E. Penner, Atmos. Oceanic Opt. **16**, Nos. 5–6, 402–410 (2003).
2. G.S. Bairashin, Yu.S. Balin, A.D. Ershov, and I.E. Penner, Nauka Proizvodstvu, No. 6 (2003) (in print).
3. G.I. Galazii, *Baikal in Questions and Answers*, http://www.icc.ru/gal/index.html.
4. V.E. Zuev, V.V. Antonovich, B.D. Belan, E.F. Zhbanov, M.K. Mikushev, M.V. Panchenko, A.V. Podanev, G.N. Tolmachev, and A.V. Shcherbatova, Dokl. Ros. Akad. Nauk **325**, No. 6, 1146–1150 (1992).
5. M.Yu. Arshinov, B.D. Belan, G.A. Ivlev, T.M. Rasskazchikova, Atmos. Oceanic Opt. **14**, No. 4, 263–266 (2001).
6. Yu.A. Israel and Yu.A. Anokhin, eds., *Monitoring of the State of Lake Baikal* (Gidrometeoizdat, Leningrad, 1991), 238 pp.
7. P.P. Sherstyankin, L.N. Kuimova, and R.E. Minenko, Dokl. Ros. Akad. Nauk **345**, No. 2, 251–255 (1995).
8. S.K. Guleev and E.B. Tonkacheev, Dokl. Ros. Akad. Nauk **326**, No. 2, 371–375 (1992).
9. V.E. Zuev, B.D. Belan, and G.O. Zadde, *Optical Weather* (Nauka, Novosibirsk, 1990), 192 pp.
10. Yu.S. Balin and A.D. Ershov, Atmos. Oceanic Opt. **13**, Nos. 6–7, 586–591 (2000).
11. A.K. Khrgian, *Atmospheric Physics* (Gidrometeoizdat, Leningrad, 1978), Part 2, 319 pp.
12. R.G. Barry, *Weather and Climate in Mountains* (Gidrometeoizdat, Leningrad, 1984), 310 pp.
13. R.S. Scorer, *Environmental Aerodynamics* (Ellis, Horwood, Chichester, 1978).
14. Sh.A. Musaelyan, *Obstacle Waves in the Atmosphere* (Gidrometeoizdat, Leningrad, 1962), 125 pp.
15. A.E. Gill, *Atmosphere–Ocean Dynamics* (Academic Press, 1982).
16. V.K. Arguchintsev, A.V. Arguchintseva, and M.A. Kreisik, Atmos. Oceanic Opt. **14**, No. 3, 216–218 (2001).
17. A.A. Baklanov, *Modeling of the Dynamics and Pollution of the Atmosphere in Northern Regions with Complex Orography*, http://alphais.inep.ksc.ru/tezis7.html.
18. N.M. Astaf'eva, Usp. Fiz. Nauk **166**, No. 11, 1145–1170 (1996).
19. V.I. Vorob'ev and V.G. Gribunin, *Theory and Practice of Wavelet Transform* (VUS, Saint Petersburg, 1999), 203 pp.
20. I.M. Dremin, O.V. Ivanov, and V.A. Nechitailo, Usp. Fiz. Nauk **171**, No. 5, 465–501 (2001).
21. V.P. D'yakonov, *Wavelets. From Theory to Practice* (R-Solon, Moscow, 2002), 440 pp.
22. http://www.matlab.ru/wavelet/b[18]k1/3/scal2frq.asp
23. J. Lewall, *Tutorial on Continuous Wavelet Analysis of Experimental Data*, http://www.mame.syr.edu/faculty/lewalle/tutor/tutor.html.
24. B.D. Belan, Atmos. Oceanic Opt. **7**, No. 8, 558–562 (1994).
25. *Territorial Complex Scheme for Lake Baikal Basin Nature: Protection of Main Principles* (Giprogor, Moscow, 1990), Part 1, 303 pp.